

Electronic structure of donor states under a strong magnetic field

G. M. Huang, Y. M. Liu, and C. G. Bao*

The State Key Laboratory of Optoelectronic Materials and Technologies, and Department of Physics, Zhongshan University, Guangzhou, 510275, People's Republic of China

(Received 16 August 2004; published 2 February 2005)

The electronic structures of quantum dots with 6, 9, and 13 electrons under the influence of a strong magnetic field together with a positive impurity has been studied. By diagonalizing the Hamiltonian and by a detailed analysis of the wave functions, both crystal-like and liquidlike states were found. The crystal-like states have clear core-ring structures. The effect of impurity and the effect of symmetry constraint on these structures has been clarified. Based on the symmetry constraint, the states can be well classified, and the candidates of magic angular momenta can be predicted.

DOI: 10.1103/PhysRevB.71.075302

PACS number(s): 71.27.+a

I. INTRODUCTION

It is well known that the quantum dots as a kind of artificial microstructures are important and attractive from both the application and academic points of view.¹⁻¹² The superiority of quantum dots arises mainly from the fact that their properties can be controlled. Various kinds of dots can be made for various purposes. Due to the diversity, very rich physics is involved. In the theoretical aspect, there are a number of effective theoretical methods, e.g., the Hartree-Fock method,¹³ the “exact diagonalization” method,¹⁴ and the density-functional approach.^{10,15} When the number of electrons N in a dot is neither few nor many (say, $6 \leq N \leq 50$), the core-ring model of electronic structure is believed to be reasonable.¹⁶⁻¹⁹ The existence of such a picture has been revealed by numerical calculation and studied in detail in recent works.²⁰⁻²²

On the other hand, electric and magnetic field are usually used for controlling. In addition, the deposition of an impurity can affect the electronic structures severely, therefore this is also a way for controlling. The effect of the electronic and magnetic field has already been widely studied, but the effect of impurity is less studied.²³⁻²⁷

Furthermore, since each quantum state is required to transform in a specific way under rotation, inversion, and particle permutation, the structure of the wave function is therefore constrained by this requirement. It turns out that the symmetry constraint might lead to the appearance of inherent nodes, thus the stability of the quantum state is seriously affected. This fact imposes a strong impact on low-lying spectra, in particular, the series of magic angular momenta is decisively affected. However, the combined effect of symmetry constraint and impurity has not yet been concerned.

As a continuation of the previous study, this paper is dedicated to study further the effect of impurity on the core-ring structures. A positive impurity is placed at the center of the dot, and a strong magnetic field is applied. Only the polarized states with the filling factor $\nu \leq 1$ are concerned. By diagonalizing the Hamiltonian with the basis functions including not only the lowest Landau level (LLL) but also higher levels, and by a detailed analysis of the wave functions, the combined effect of impurity and symmetry constraint has been exhibited.

II. HAMILTONIAN AND THE APPROACH

Let the electrons be confined in a X - Y plane by a parabolic confinement. The Hamiltonian reads

$$H = - \sum_{j=1}^N \frac{\hbar^2}{2m^*} \nabla^2 + U - \frac{\hbar\omega_c}{2} L, \quad (1)$$

$$U = \sum_{j=1}^N \frac{1}{2} m^* \omega^2 r_j^2 + \frac{e^2}{4\pi\epsilon_0\epsilon_r} \sum_{j < k} \frac{1}{r_{jk}} - \sum_{j=1}^N \frac{Ze^2}{4\pi\epsilon_0\epsilon_r r_j},$$

$$\omega_0 = \left(\omega_0^2 + \frac{\omega_c^2}{4} \right)^{1/2}, \quad \omega_c = \frac{eB}{m^*c},$$

where $m^* = 0.067m_e$ is the effective electron mass for a GaAs dot, L is the total orbital angular momentum, Ze is the charge of the impurity ($Z=1$ is assumed in the following), B is the magnetic field perpendicular to the X - Y plane ($B=10$ T is assumed), $\epsilon_r = 12.4$ is the background dielectric constant, and \mathbf{r}_j the position vector of the j th electron ($r_{jk} = |\mathbf{r}_j - \mathbf{r}_k|$). $\hbar\omega_0 = 3$ meV measures the strength of the parabolic confinement. The small Zeeman term has been neglected. Since only the polarized states are considered, the spatial wave functions are completely antisymmetrized and the spin-part can be omitted.

The Schrödinger equation was solved using the same method as stated in Ref. 21. Comparing with other methods of diagonalizing the Hamiltonian, our method has three features. (1) The basis functions (BFs) contain a variational parameter, thereby they can be optimized. (2) The BFs are ordered in such a sequence so that the one with a smaller index is more important to low-lying states. With such a sequence, the Hamiltonian matrix can be enlarged step by step until a satisfactory convergency has been achieved. (3) In addition to the BFs belonging to the lowest Landau levels, a part of higher levels are included. Thus our method is in general an improvement of those suffering the LLL limitation.

Let a series of states having the same L be denoted as $(L)_i$, where the $i=1$ state is the lowest and is called a first state. The corresponding eigenenergy is denoted as $E[(L)_i]$. To

TABLE I. The energies (in meV) of the first states $E[(L)_1]$. The first row is the number of basis functions used in the calculation.

	10 000	11 000	12 000
$E[(21)_1] (N=6)$	258.390	258.381	258.375
$E[(82)_1] (N=13)$	1069.951	1069.881	1069.842

show the convergency of our calculation, examples for $N=6$ and 13 systems are given in Table I.

From Table I, one can see that the convergency is not very good. However, it was found that the densities, as defined later, extracted from the wave functions obtained by using 10 000, 11 000, and 12 000 BFs are nearly indistinguishable. Since we are only interested in the qualitative aspect, the accuracy achieved by using 12 000 BFs is sufficient for our purpose.

It is noted that, for a first state, if the Coulomb interaction (the last two terms in U) is removed from the Hamiltonian, all the electrons will fall in the LLL with the energy $(L+N)\hbar\omega - (\hbar\omega_c/2)L$. Let us define

$$\varepsilon(L) \equiv E[(L)_1] - (L+N)\hbar\omega + \frac{\hbar\omega_c}{2}L. \quad (2)$$

This quantity is a measure of the Coulomb repulsion in the first states.

Let the eigenwave functions be denoted as Ψ_L . For studying the electronic structures, we define the one-body density as

$$\rho_1(\mathbf{r}_1) = \int |\Psi_L|^2 d\mathbf{r}_2 d\mathbf{r}_3 \cdots d\mathbf{r}_N \quad (3)$$

and the two-body density as

$$\rho_2(\mathbf{r}_1, \mathbf{r}_2) = \int |\Psi_L|^2 d\mathbf{r}_3 d\mathbf{r}_4 \cdots d\mathbf{r}_N. \quad (4)$$

These functions will be inspected.

III. CORE-RING STRUCTURES AND SYMMETRY CONSTRAINTS

It was found that the core-ring structures of electrons are realistic,^{20,21} where N_{out} electrons are contained in the ring outside while the rest $N_{\text{in}}=N-N_{\text{out}}$ are contained in the core inside. It can be further assumed that the ring contains an angular momentum l_{out} while the core contains $l_{\text{in}}=L-l_{\text{out}}$. Obviously, both N_{out} and l_{out} are not good quantum numbers. Therefore, in general, the spatial wave function can be expanded as

$$\Psi_L = \tilde{A} \sum_{\beta, l_{\text{out}}, N_{\text{out}}} C_{l_{\text{out}}, N_{\text{out}}}^{\beta} F_{l_{\text{in}}, N_{\text{in}}}^{\beta, \text{core}} F_{l_{\text{out}}, N_{\text{out}}}^{\beta, \text{ring}}, \quad (5)$$

where $F_{l_{\text{out}}, N_{\text{out}}}^{\beta, \text{ring}}$ is itself an antisymmetrized function of the N_{out} electrons with the angular momentum l_{out} , and is mainly distributed in the ring. β is introduced to respond to the possibility that this function may not be unique. Whereas

$F_{l_{\text{in}}, N_{\text{in}}}^{\beta, \text{core}}$ is for the N_{in} electrons mainly distributed in the core. $C_{l_{\text{out}}, N_{\text{out}}}^{\beta}$ are the coefficients of combination and \tilde{A} is the antisymmetrizer. Although neither l_{out} nor N_{out} is a good quantum number, a specific pair of them might be dominant, as we shall see.

Let us first study the symmetry constraints imposing on the component $F_{l_{\text{out}}, N_{\text{out}}}^{\beta, \text{ring}}$. When the N_{out} electrons turn out to form a regular polygon, a rotation by $2\pi/N_{\text{out}}$ is equivalent to a cyclic permutation of electrons. This equivalence leads to an equation of constraint

$$e^{-i2\pi l_{\text{out}}/N_{\text{out}}} F_{l_{\text{out}}, N_{\text{out}}}^{\beta, \text{ring}} = \pm F_{l_{\text{out}}, N_{\text{out}}}^{\beta, \text{ring}} \quad (6)$$

valid at the polygon, the left side arises from the rotation, and the right side from the permutation. The plus (negative) sign would be taken if N_{out} is odd (even). Thus, if N_{out} is odd (even) and if $l_{\text{out}}/N_{\text{out}}$ is not an integer (half integer), $F_{l_{\text{out}}, N_{\text{out}}}^{\beta, \text{ring}}$ would be zero at the polygon, i.e., an inherent node would emerge. In other words, when the requirement

$$l_{\text{out}} = N_{\text{out}}\{j + [1 + (-1)^{N_{\text{out}}}/4]\} \quad (7a)$$

does not hold (where j is an arbitrary integer), the N_{out} -sided regular polygon is forbidden, and the inherent node would cause an increase of energy. In this case the component $F_{l_{\text{out}}, N_{\text{out}}}^{\beta, \text{ring}}$ is not advantageous to binding, and therefore would not be important to low-lying states.

Similarly, if

$$l_{\text{in}} = N_0\{j + [1 + (-1)^{N_0}/4]\} \quad (7b)$$

does not hold (where $N_0=N_{\text{in}}$ or $=N_{\text{in}}-1$; in the latter case, an electron stays at the center), the N_0 -sided smaller regular polygon is forbidden, and accordingly $F_{l_{\text{in}}, N_{\text{in}}}^{\beta, \text{core}}$ is not important.

Equations (7a) and (7b) serve to discriminate the important components in the first states. If a couple l_{out} and N_{out} can be found fulfilling Eq. (7a) while at the same time the associated l_{in} and N_0 fulfill Eq. (7b), and if the associated core-ring configuration (having N_{out} electrons in the ring and N_{in} in the core) is lower in total potential energy U , then the associated component $F_{l_{\text{in}}, N_{\text{in}}}^{\beta, \text{core}} F_{l_{\text{out}}, N_{\text{out}}}^{\beta, \text{ring}}$ would be relatively more important in the expansion of Eq. (5). If there is no other important component to compete, the only important component alone would be dominant and the first-state $(L)_1$ would have a clear core-ring structure. In particular, if the associated core-ring configuration is specially low in U , the associated $L=l_{\text{in}}+l_{\text{out}}$ is a candidate of magic number, and the associated first state is a candidate of the true ground state.

The above discussion is a base to understand the following results. Incidentally, since the moment of inertia of the core is much smaller than that of the ring, l_{in} is much smaller than l_{out} in lower states. Otherwise, the collective rotation energy will greatly increase. A better choice is to have l_{in} as least as possible (allowed by Pauli principle) as²²

$$l_{\text{in}} = (l_{\text{in}})_{\text{min}} = N_{\text{in}}(N_{\text{in}} - 1)/2. \quad (7c)$$

It was found that this is the case for all the first-states unless L is very large.²⁰⁻²² In this case the core is said to be

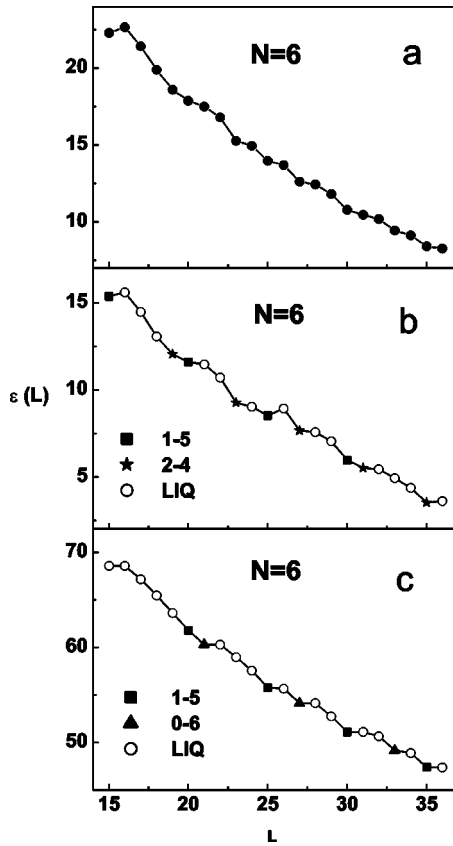


FIG. 1. $\varepsilon(L)$ (in meV) as a function of L with $N=6$, $B=10$ T, and $Z=1$ (a and b) or $Z=0$ (c). The LLL limitation is imposed in (a), but not in (b) and (c). In the two latter cases the number of the basis function is 12 000.

inert. It is straightforward to prove that $(l_{in})_{min}$ satisfies Eq. (7b) automatically. In what follows, we shall use Eq. (7c) to replace Eq. (7b).

IV. ELECTRONIC STRUCTURES OF DONOR STATES OF $N=6$ DOTS

In what follows the results of the first states are given. We use meV and $a_M \equiv \sqrt{\hbar/m^* \omega} = 111.51 \text{ \AA}$ (if $B=10$ T) as the units of energy and length. Let us first inspect $\varepsilon(L)$ given in Fig. 1, where Fig. 1(a) results from the diagonalization containing only the BFs of LLL (the number of this kind of BFs is 1 if $L=15$, 35 if $L=25$, and 282 if $L=35$). However, in addition to all the LLL, totally 12 000 BFs are used for Fig. 1(b). Thus the effect of higher Landau levels is revealed by comparing Fig. 1(a) with 1(b). It was found that the inclusion of higher levels leads to a decrease of energy about

5 to 7 meV, thus the effect of the higher levels on energy is not negligible. Nonetheless, the effect becomes smaller if L is larger. In addition, although the curves in Figs. 1(a) and 1(b) have the same tendency, some details have been changed. For example, $\varepsilon(26)$ is remarkably higher in (b) but not in (a), and $\varepsilon(35)$ is remarkably lower in (b) but not so much in (a), etc. To see the effect of higher Landau levels on the structure of wave function, let us evaluate the weights of the LLL (W_{LLL}) in the wave functions obtained from our calculation with 12 000 BFs. They are listed in Table II for some selected states.

From this table it is clear that the weights of higher levels are not very small, therefore the inclusion of higher Landau levels is necessary, in particular if a positive impurity exists. In order to understand the physics involved in Fig. 1, we have to investigate the electronic structures by analyzing the wave functions. It was found that there are three types of state. The first type has a clear core-ring structure with $N_{out}=5$ (and accordingly $N_{in}=1$), this is called a 1-5 structure and is marked by a black square in Fig. 1(b). Examples of this type are given in Figs. 2(a), 2(b), 3(a), and 3(b). The ρ_1 in Fig. 2(a) has a minimum at $r=r_0=1.14$, r_0 can be considered as the border separating the core and the ring. It was found that

$$2\pi N \int_{r_0}^{\infty} \rho_1(r) r dr = 4.88. \quad (8)$$

The ρ_1 in Fig. 2(b) has $r_0=1.52$ and the corresponding integration gives 4.77. Both values are close to 5, thus they support the suggestion of having the 1-5 structure. The ρ_2 in Figs. 3(a) and 3(b) have a core, and have one electron together with two peaks in the upper-half ring, thus they confirm directly the existence of the 1-5 structure. Since the wave function is meanwhile distributed sharply surrounding a symmetric geometric structure (a centered pentagon), this structure is said to be crystal-like.

The second type has a 2-4 structure and is marked by a star in Fig. 1(b). The ρ_1 in Figs. 2(c) and 2(d) have $r_0=1.70$ and 1.88, the corresponding integrations [see Eq. (8)] give 4.11 and 4.06. These data support the suggestion of having the 2-4 structure. The ρ_2 in Figs. 3(c) and 3(d) have a core, and have one electron together with two peaks in the upper-half ring, thus they confirm directly the existence of the 2-4 crystal-like structure.

Instead of being crystal-like, the third type is liquidlike and is marked by a white circle in Fig. 1(b), they do not have a clear geometric feature. Examples are given in Figs. 2(e) and 2(f), where the border between the core and the ring cannot be well defined. Accordingly, in Figs. 3(e) and 3(f), a crystal-like picture no longer exists.

TABLE II. Weights of the LLL (W_{LLL}) in the first states with (upper row) and without (lower row) the impurity

	$(L)_1$	$(15)_1$	$(20)_1$	$(25)_1$	$(30)_1$	$(35)_1$
with impurity		0.7002	0.7260	0.7896	0.8174	0.8299
without		0.6839	0.7289	0.8748	0.9007	0.9192

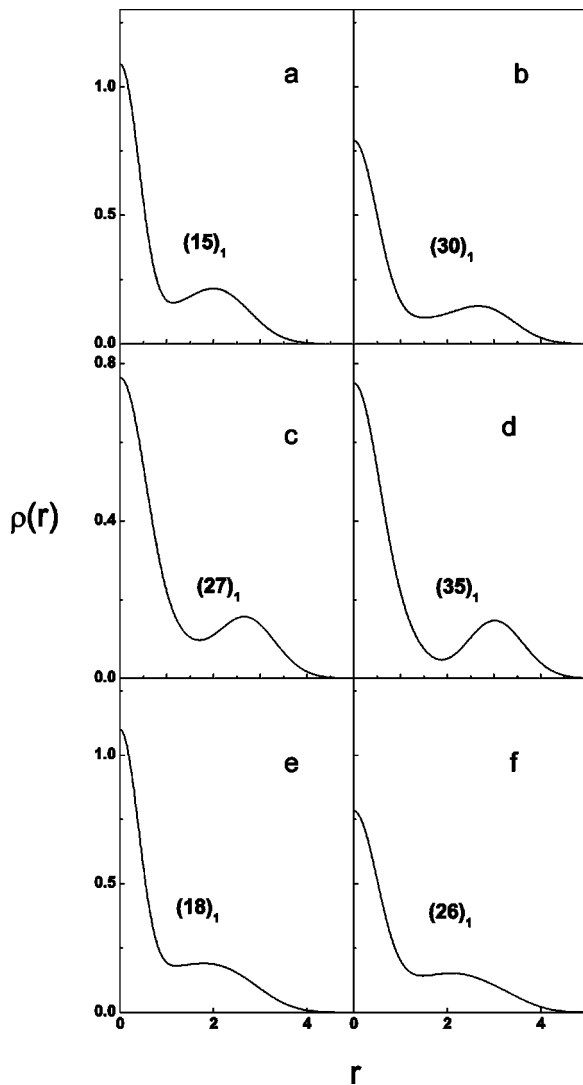


FIG. 2. $\rho_1(r)$ of the first states as a function of r . $N=6$, $B=10$ T and $Z=1$ are given. The labels of state $(L)_1$ are marked in the subfigures.

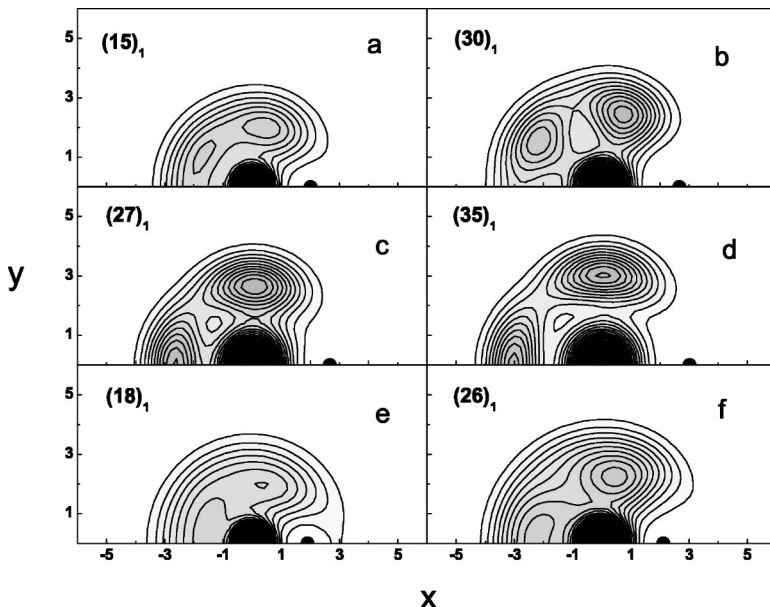


FIG. 3. Contour diagrams of $\rho_2(\mathbf{r}_1, \mathbf{r}_2)$ as a function of \mathbf{r}_1 plotted in the upper half X - Y plane. \mathbf{r}_2 is fixed and is marked by a black spot at the X axis. $N=6$, $B=10$ T, and $Z=1$ are given. The darker area is larger in magnitude. The labels of state $(L)_1$ are marked.

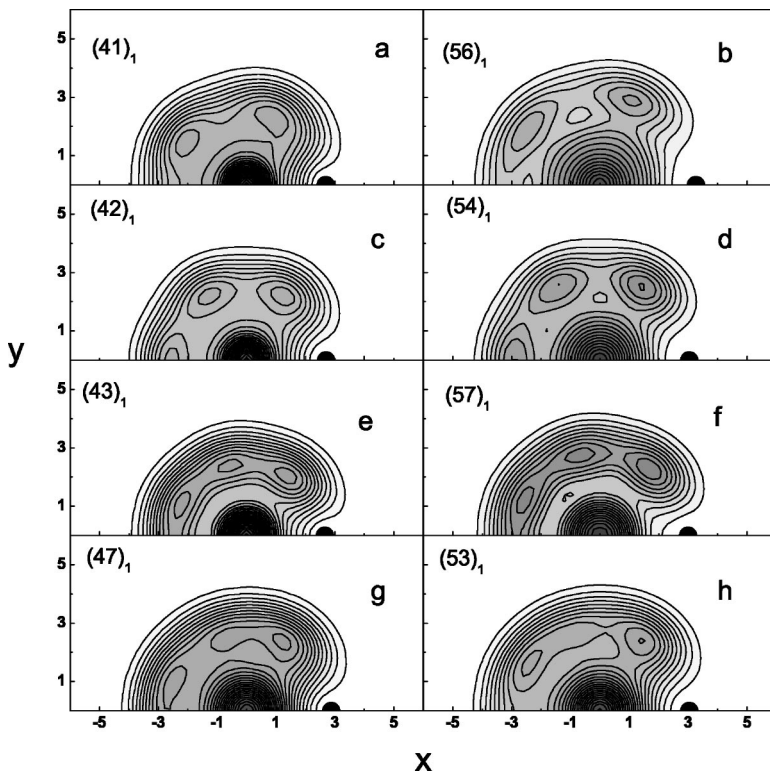
It is noted that the impurity acts as an attractive center. If an electron is close to the center with angular momentum zero, the attractive electron-impurity interaction will be strengthened. However, if too many electrons are close to the center, they will strongly repulse each other. It was found that, when $N=6$, the case with $N_{in} \geq 3$ is not advantageous to binding. On the other hand, the 1-5 and the 2-4 structures are lower in total potential energy, and they would be pursued if the requirement (7) can be satisfied. It turns out that all the states of type one have L as a multiple of 5 (i.e., $L=5j$). For these states if the angular momentum and the particles are divided as $l_{out}=5j$ and $N_{out}=5$, and accordingly $l_{in}=0$ and $N_{in}=1$, then the requirement (7) can be satisfied. Thus, these $L=5j$ states are allowed by symmetry to pursue the favorable 1-5 structure, and their first states actually possess this structure without exception.

All the states with $L=4j+3$ belong to the second type. For these states, if the angular momentum and the particles are divided as $l_{out}=4j+2$ and $N_{out}=4$, and accordingly $l_{in}=1$ and $N_{in}=2$, then the requirement (7) is met. Thus, these states are allowed by symmetry to pursue the 2-4 structure, and their first states actually possess this structure without exception.

For the states with $L=5j=4j'+3$ (e.g., $L=15, 35, 55, \dots$), both the 1-5 and 2-4 structures are accessible to them. There is a competition between these two structures. It turns out that the 2-4 structure is mostly the winner (with one exception as stated below). For example, the $(35)_1$ state has a clear 2-4 structure as shown in Fig. 3(d).

The $(15)_1$ state is very special because it has the filling factor $\nu=1$, accordingly it has only one BF belonging to the LLL. It is noted that a clear geometric structure arises from the interference of a number of BFs. Since the one of the LLL can not interfere effectively with other BFs of higher levels, the geometric feature of $(15)_1$ would be ambiguous. It turns out that this state has an ambiguous 1-5 structure as shown in Fig. 3(a).

For all the first states with $L \neq 5j$ and $L \neq 4j+3$, no superior structure can be pursued. They might be a mixture of

FIG. 4. The same as Fig. 3 but for $N=9$.

many structures, and appear liquidlike as shown in Figs. 3(e) and 3(f).

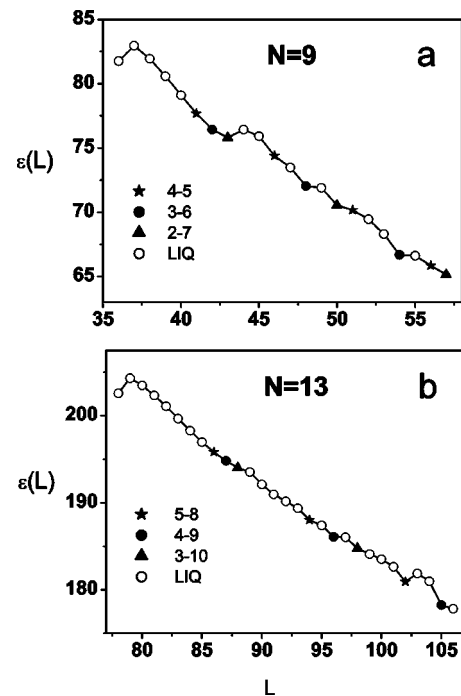
From the above discussion, it is clear that the classification of states is closely related to symmetry constraint.^{28,29} Since the 1-5 and 2-4 structures are associated with a lower U , accordingly the types one and two are lower in $\varepsilon(L)$ as shown in Fig. 1(b). They are candidates of the ground states, the L of them are candidates of the magic numbers.

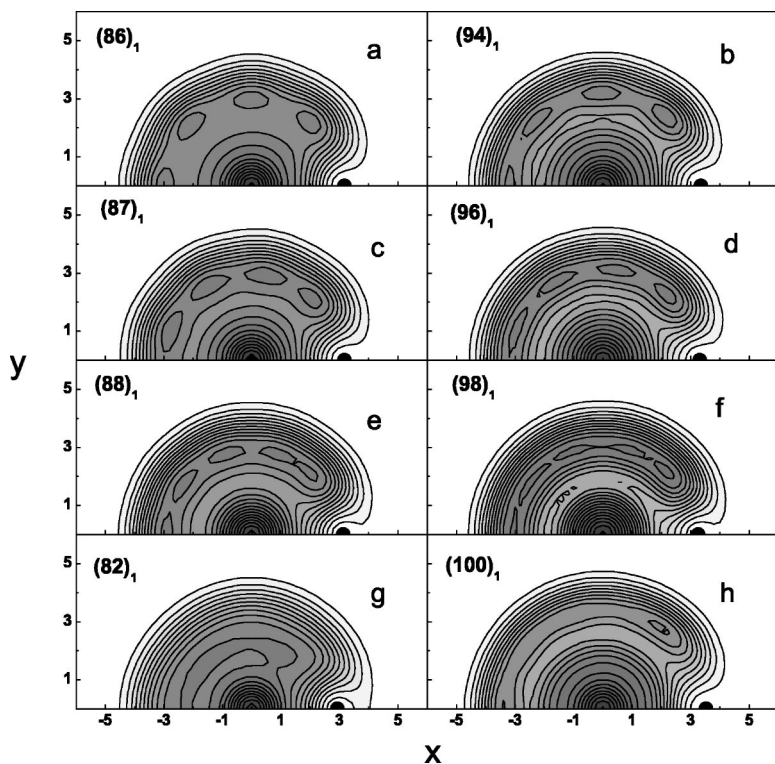
When the impurity is removed, the 2-4 structure is no more advantageous due to the strong Coulomb repulsion of the two inner electrons without the overcompensation of the attraction from the impurity. Instead, the 0-6 structure competes with the 1-5 structure. The $\varepsilon(L)$ of this case is plotted in Fig. 1(c), where the associated states are also classified into three types. The first type has the 1-5 structure, the second has the 0-6 structure, while the third is liquidlike.²⁰ Comparing Fig. 1(c) with 1(b), the black squares appear at the same places, i.e., $L=5j$. The black star in Fig. 1(b) does not appear in 1(c), instead the black triangles appear when $L=6j+3$ ($l_{\text{out}}=L$ and $N_{\text{out}}=6$). Note that a hexagon is accessible only to the $L=6j+3$ states. This finding confirms once more the decisive effect of symmetry constraint. Due to the appearance of the 0-6 structure to replace the 2-4, the series of magic numbers in the cases with and without impurity are different. For example, the $(23)_1$ state is low in Fig. 1(b) but high in Fig. 1(c).

V. ELECTRONIC STRUCTURES OF DONOR STATES OF $N=9$ DOTS

From a consideration of classical dynamics, when a positive impurity is present, the favorable structures of $N=9$ dots

are the 2-7, 3-6, and 4-5 (in a sequence of increasing U). From a consideration of symmetry constraint, the core-ring structure is allowed only if Eq. (7) is satisfied. Thus, the 2-7 is allowed if ($l_{\text{out}}=7j$ and $l_{\text{in}}=1$), i.e., $L=7j+1$. The 3-6 is allowed if ($l_{\text{out}}=6j+3$ and $l_{\text{in}}=3$), i.e., $L=6j$. The 4-5 is allowed if ($l_{\text{out}}=5j$ and $l_{\text{in}}=6$), i.e., $L=5j+6$. On the other hand, from an analysis of the wave functions, there are really

FIG. 5. The same as Fig. 1(b) but for $N=9$ (a) and for $N=13$ (b). Each figure has a group of specific types.


 FIG. 6. The same as Fig. 3 but for $N=13$.

three types of crystal-like states together with a type of liquidlike state. The angular momenta L of each type are exactly as predicted from symmetry consideration. Examples of the ρ_2 of them are given in Fig. 4, where clear 4-5, 3-6, 2-7, and liquidlike structures, respectively, are shown from the top to bottom. $\varepsilon(L)$ and the classification of states are given in Fig. 5(a), where the crystal-like structures are lower, and they are candidates of ground states.

VI. ELECTRONIC STRUCTURES OF DONOR STATES OF $N=13$ DOTS

The favorable structures from classical consideration are 3-10, 4-9, and 5-8, and they are quite close in U . Among them, the 3-10 is allowed if ($l_{\text{out}}=10j+5$ and $l_{\text{in}}=3$), i.e., $L=10j+8$. The 4-9 is allowed if ($l_{\text{out}}=9j$ and $l_{\text{in}}=6$), i.e., $L=9j+6$. The 5-8 is allowed if ($l_{\text{out}}=8j+4$ and $l_{\text{in}}=10$), i.e., $L=8j+14$. On the other hand, from an analysis of the wave functions, there are really three types of crystal-like states together with a type of liquidlike state. Again, the angular momenta of each type are exactly as predicted. Examples of

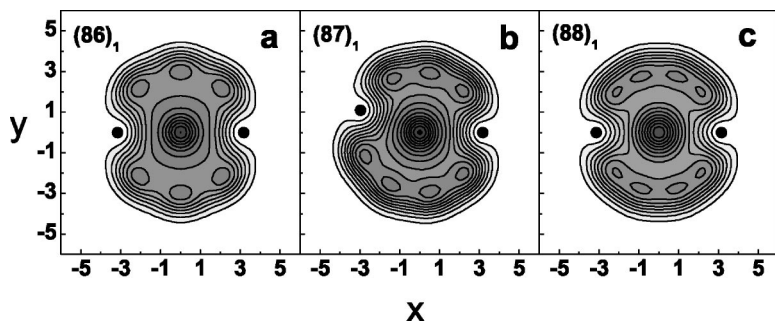
ρ_2 are given in Fig. 6, where the 5-8, 4-9, 3-10, and liquidlike structures, respectively, are shown from the top to bottom. $\varepsilon(L)$ and the classification are given in Fig. 5(b). The crystal-like picture in the ring can be revealed more clearly via the three-body densities defined as

$$\rho_3(\mathbf{r}_1, \mathbf{r}_2, \mathbf{r}_3) = \int |\Psi_L|^2 d\mathbf{r}_4 d\mathbf{r}_5 \cdots d\mathbf{r}_N. \quad (9)$$

Examples are given in Fig. 7.

VII. SUMMARY

The effect of a positive impurity on the electronic structures of the first states of $N=6, 9$, and 13 dots under a strong magnetic field has been investigated. By an analysis of the wave functions, both crystal-like and liquidlike states were found. The crystal-like states have very clear core-ring structures, and they can be further classified into types according to the number of electrons $N_{\text{out}}(N_{\text{in}})$ in the ring (core). Amazingly, it was found that, due to symmetry constraints, both N_{out} and N_{in} are matched with l_{out} and l_{in} , respectively. Con-


 FIG. 7. The three-body densities $\rho_3(\mathbf{r}_1, \mathbf{r}_2, \mathbf{r}_3)$ as a function of \mathbf{r}_1 for $N=13$ dots. The given \mathbf{r}_2 and \mathbf{r}_3 are marked by two black spots. The darker area is associated with a larger ρ_3 . $B=10$ T and $Z=1$ are assumed.

sequently, a specific core-ring structure is accessible only to the states with specific L . Thus, the types of states can be predicted. This fact demonstrates once more the decisive effect of symmetry constraint on microstructures. It was found that the crystal-like states are lower in energy; they are candidates for the ground state. Accordingly, the L of them are candidates for magic numbers.

The core ring structure has already been studied in detail in Refs. 20–22 without the impurity. With the addition of the positive impurity, the core ring structure with N_{in} a little larger would be preferred. For example, for $N=6$, the favorable structures are 0-6 and 1-5 without impurity, but they are replaced by 1-5 and 2-4 if the impurity is present. Accordingly, the magic numbers would be changed. Furthermore, when a positive impurity is contained, higher Landau levels

become more important, and therefore they are in general not negligible in numerical calculation.

This paper deals with the case with a strong magnetic field. When the field is weak, unpolarized states become important. Furthermore, when the location of impurity deviates remarkably from the center, the conservation of angular momentum breaks down, and the electronic structure becomes very complicated. This interesting topic is left for further investigation.

ACKNOWLEDGMENTS

This project was supported by the National Science Foundation of China under Grants Nos. 10174098, 10374119, and 90103028, and also by a fund from the Education Ministry of China.

*Corresponding author.

- ¹J. Weis, R. J. Haug, K. V. Klitzing, and K. Ploog, Phys. Rev. Lett. **71**, 4019 (1993).
- ²G. P. Mallon and P. A. Maksym, Physica B **256**, 186 (1998).
- ³Y. Arakawa and Y. Yariv, IEEE J. Quantum Electron. **22**, 1887 (1986).
- ⁴S. Schmitt-Rink, D. A. B. Miller, and D. S. Chemla, Phys. Rev. B **35**, 8113 (1987).
- ⁵N. Kirstaedter, N. N. Ledentsov, M. Grundmann, D. Bimberg, N. V. Ustinov, S. S. Ruvimov, M. V. Maximov, P. S. Kopev, Z. I. Alferov, U. Richter, P. Werner, U. Gosele, and J. Heydenreich, Electron. Lett. **30**, 1416 (1994).
- ⁶K. Imamura, Y. Sugiyama, Y. Nkata, S. Muto, and N. Yokoyama, Jpn. J. Appl. Phys., Part 1 **34**, L1445 (1995).
- ⁷L. Jacak, P. Hawrylak, and A. Wójs, *Quantum Dots* (Springer, Berlin, 1998).
- ⁸T. Chakraborty, *Quantum Dots* (Elsevier, Amsterdam, 1999).
- ⁹M. S. Kushwaha, Surf. Sci. Rep. **41**, 1 (2001).
- ¹⁰S. M. Reimann and M. Manninen, Rev. Mod. Phys. **74**, 1283 (2002).
- ¹¹P. A. Maksym, H. Imamura, G. P. Mallon, and H. Aoki, J. Phys.: Condens. Matter **12**, 299 (2000).
- ¹²S. Tarucha, D. G. Austing, T. Honda, R. J. vander Haage, and L. Kouwenhoven, Phys. Rev. Lett. **77**, 3613 (1996).
- ¹³D. Pfannkuche, V. Gudmundsson, and P. A. Maksym, Phys. Rev. B **47**, 2244 (1993).
- ¹⁴T. Chakraborty, *Quantum Dots: A Survey of the Properties of Artificial Atoms* (North-Holland, Amsterdam, 1999).
- ¹⁵G. Vignale and M. Rasolt, Phys. Rev. Lett. **59**, 2360 (1987); Phys. Rev. B **37**, 10 685 (1988).
- ¹⁶C. de C. Chamon and X. G. Wen, Phys. Rev. B **49**, 8227 (1994).
- ¹⁷H. M. Muller and S. E. Koonin, Phys. Rev. B **54**, 14 532 (1996).
- ¹⁸E. Goldmann and S. R. Renn, Phys. Rev. B **60**, 16 611 (1999).
- ¹⁹S. M. Reimann, M. Koskinen, M. Manninen, and B. R. Mottelson, Phys. Rev. Lett. **83**, 3270 (1999).
- ²⁰C. G. Bao, J. Phys.: Condens. Matter **14**, 8549 (2002).
- ²¹G. M. Huang, Y. M. Liu, and C. G. Bao, Phys. Rev. B **68**, 165334 (2003).
- ²²G. M. Huang, Y. M. Liu, and C. G. Bao (unpublished).
- ²³K. S. Chan, H. P. Ho, E. Y. B. Pun, and W. Y. Ruan, Commun. Theor. Phys. **35**, 735 (2001).
- ²⁴K. S. Chan and W. Y. Ruan, J. Phys.: Condens. Matter **13**, 5799 (2001).
- ²⁵J. Z. Garcia, P. Pietilainen, and P. Hyvonen, Phys. Rev. B **66**, 195324 (2002).
- ²⁶C. Riva, V. A. Schweigert, and F. M. Feeters, Phys. Rev. B **57**, 15 392 (1998).
- ²⁷V. Halonen, P. Hyvonen, P. Pietilainen, and T. Chakraborty, Phys. Rev. B **53**, 6971 (1996).
- ²⁸W. Y. Ruan, Y. Y. Liu, C. G. Bao, and Z. Q. Zhang, Phys. Rev. B **51**, 7942 (1995).
- ²⁹C. G. Bao, Phys. Rev. Lett. **79**, 3475 (1997).